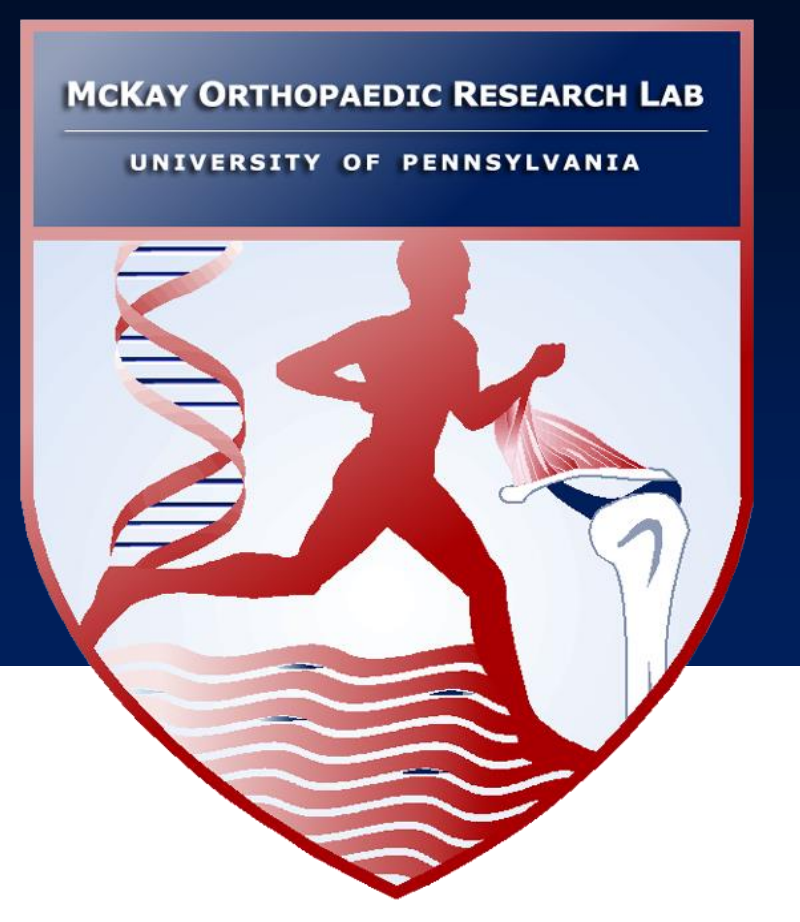


# Greater Activation of Modeling-Based Bone Formation and Improvement in Bone Microarchitecture by Intermittent PTHrP vs. PTH in Ovariectomized (OVX) Rats



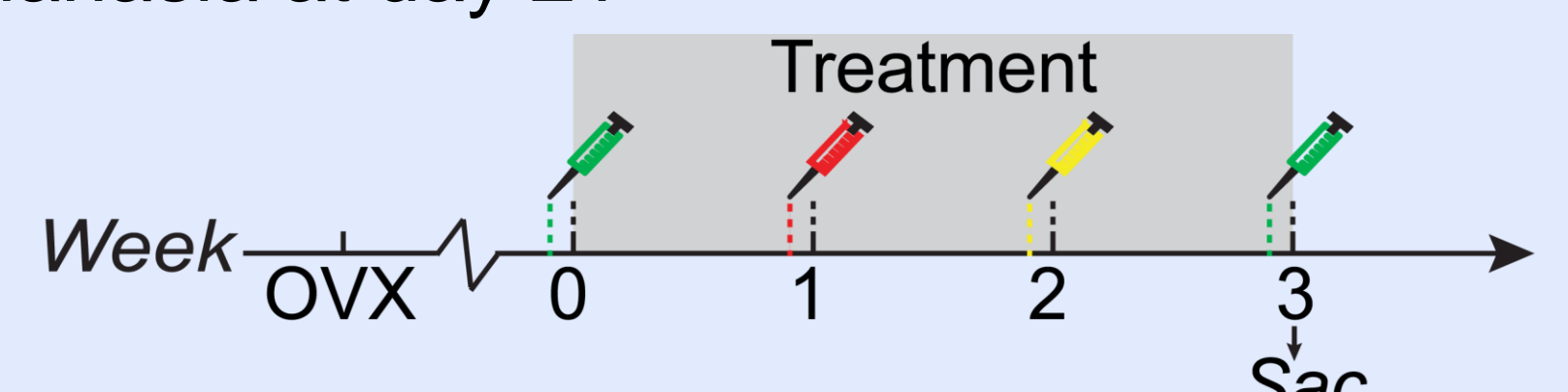
Tala Azar, Wenzheng Wang, Wei-Ju Tseng, Hongbo Zhao, Nathaniel Dyment, X. Sherry Liu

McKay Orthopaedic Research Laboratory, Department of Orthopaedic Surgery, University of Pennsylvania, Philadelphia, PA

## Introduction

- **Intermittent parathyroid hormone (PTH) and PTH related peptide (PTHrP)**
  - FDA-approved anabolic agents for osteoporosis
  - Induce modeling- and remodeling- based bone formation [1]
- **Modeling-based bone formation (MBF)**
  - Bone formation on quiescent bone surface without prior activation of bone resorption [2]
  - Only naturally occurring during growth, healing, and with external mechanical loading in adult skeleton [3]
- **Remodeling-based bone formation (RBF)**
  - Bone resorption followed by new bone formation over resorbed surfaces [2]
  - Constantly occurring to maintain a healthy skeleton [3]
- **Objective:** To compare the efficacy of PTH and PTHrP by assessing their effects on trabecular bone microarchitecture and their ability to induce MBF and RBF
- **Hypothesis:** Different levels of MBF and RBF induced by PTHrP vs. PTH may lead to different degrees of improvement in bone microarchitecture

## Materials and Methods

- **Animal protocol:** Sprague-Dawley (SD) rats received bilateral OVX surgery at 4 months of age and developed osteopenia for 12 weeks
  - **Treatment:** 40µg/kg/day for µCT study and 20µg/kg/day for histomorphometry study; 5x/wk for 3 weeks
    - **VEH:** n=15/6 for µCT/histomorphometry, saline
    - **PTH:** n=36/6 for µCT/histomorphometry, PTH 1-34
    - **PTHrP:** n=17/6 for µCT/histomorphometry, PTHrP 1-36
  - **In vivo µCT:** Metaphysis of the right proximal tibia (Fig. 1A)
    - 10.5 µm voxel size by Scanco vivaCT 40 at wk 0 & wk 3
    - Trabecular bone volume fraction (BV/TV), trabecular thickness (Tb.Th), trabecular separation (Tb.Sp), trabecular number (Tb.N), connectivity density (Conn.D), structural model index (SMI)
  - **Multicolor fluorochrome injections for histomorphometry:** (calcein/green/G, alizarin complexone/red/R, tetracycline/yellow/Y)
    - Sequence of G-R-Y-G at days -2, 5, 12, 19
    - Euthanasia at day 21
- 
- **Cryohistomorphometry and imaging:** 8µm cryosections of the proximal tibia underwent multiple rounds of imaging
    - Darkfield and fluorescent microscope → Trabecular structure and multi-color fluorochrome labels (Fig. 2A-C)
    - Polarizing microscope (decalcified sections) → Cement line and surrounding collagen fibers
  - **Identification of MBF and RBF sites**
    - **MBF:** Smooth cement line and uniform surrounding collagen fibers (Fig. 2D)
    - **RBF:** Scalloped cement line with interrupted collagen fibers (Fig. 2E)
  - **Dynamic histomorphometry analysis:** mineralizing surface (MS/BS), mineral apposition rate (MAR), and bone formation rate (BFR/BS)

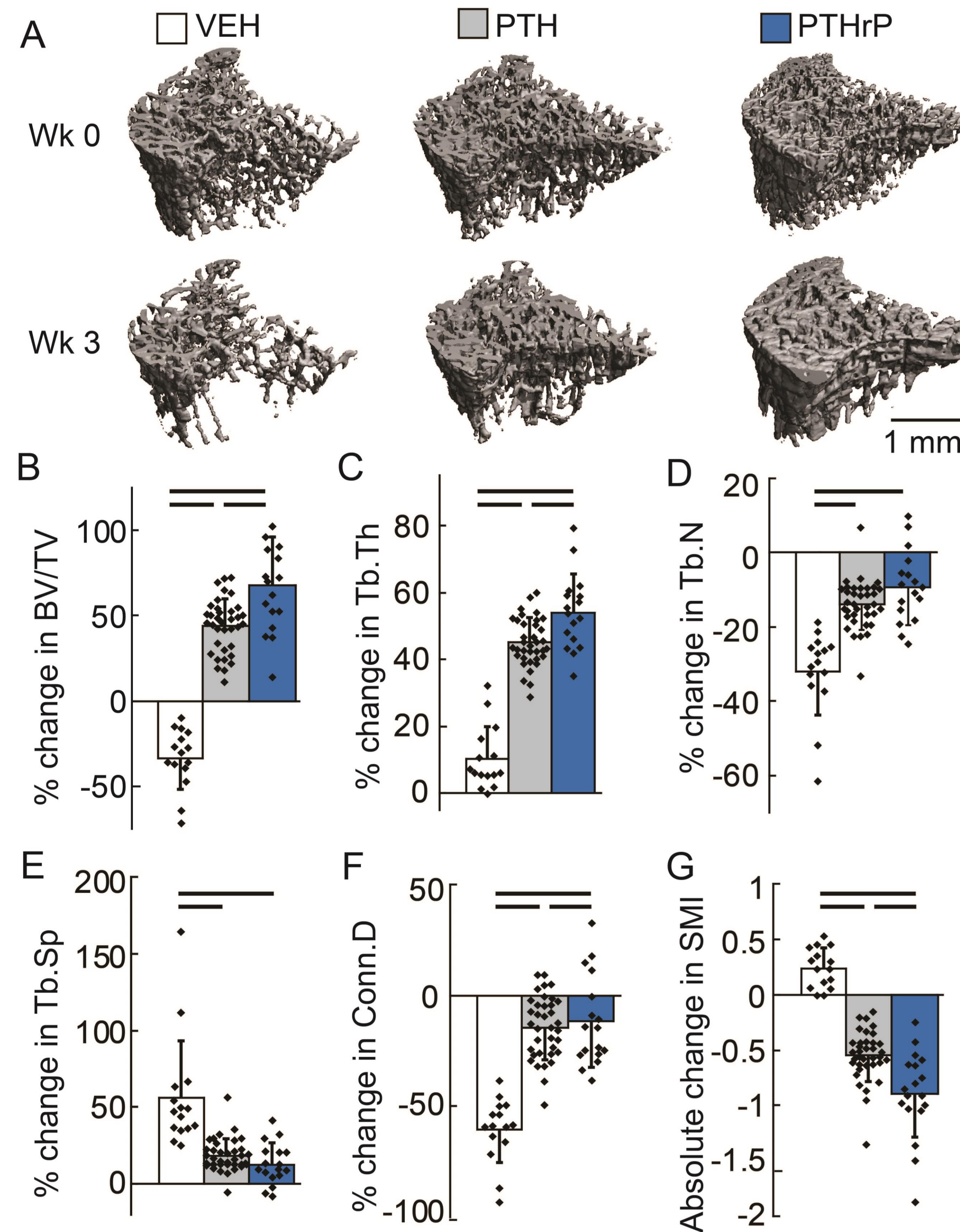


**Fig.1** (A) Representative 3D images of trabecular bone microarchitecture of the proximal tibia at baseline (wk 0) and end of treatment regimen (wk 3). (B-F) % change in (B) BV/TV, (C) Tb.Th, (D) Tb.N, (E) Tb.Sp, and (F) Conn.D. (G) Absolute change in SMI. Bar:  $p < 0.05$  by one-way ANOVA.

## Results

### In vivo µCT (Fig. 1B-G)

- **Effects of VEH treatment**
  - Reduction in BV/TV, Tb.N, Conn.D, and plate-like trabeculae (increased SMI)
  - Increase in Tb.Th and Tb.Sp
- **Effects of PTH/PTHrP treatment**
  - Improvements in BV/TV, Tb.Th, and plate-like trabeculae (decreased SMI)
  - Less reduction in Tb.N and Conn.D and attenuated increase in Tb.Sp compared to VEH
- **Effects of PTHrP vs. PTH, respectively**
  - Greater improvement in BV/TV (68% vs. 44%) and Tb.Th (54% vs. 45%)
  - Less reduction in Conn.D (-12% vs. -14%)
  - Greater increase in plate-like trabeculae (-0.9 vs. -0.6 in SMI)
  - No difference in % reduction of Tb.N between PTH (-14%) and PTHrP (-9%)

### Histomorphometry (Fig. 2F-H)

- **Effects of PTH/PTHrP treatment**
  - Greater MBF- and RBF-induced MS/BS, MAR, and BFR/BS compared to VEH treatment
- **Effect of PTHrP vs. PTH treatment, respectively**
  - 55% and 50% greater MBF-induced MS/BS and BFR/BS
  - No difference in MAR
  - Similar increase of RBF-induced MS/BS, MAR, and BFR/BS

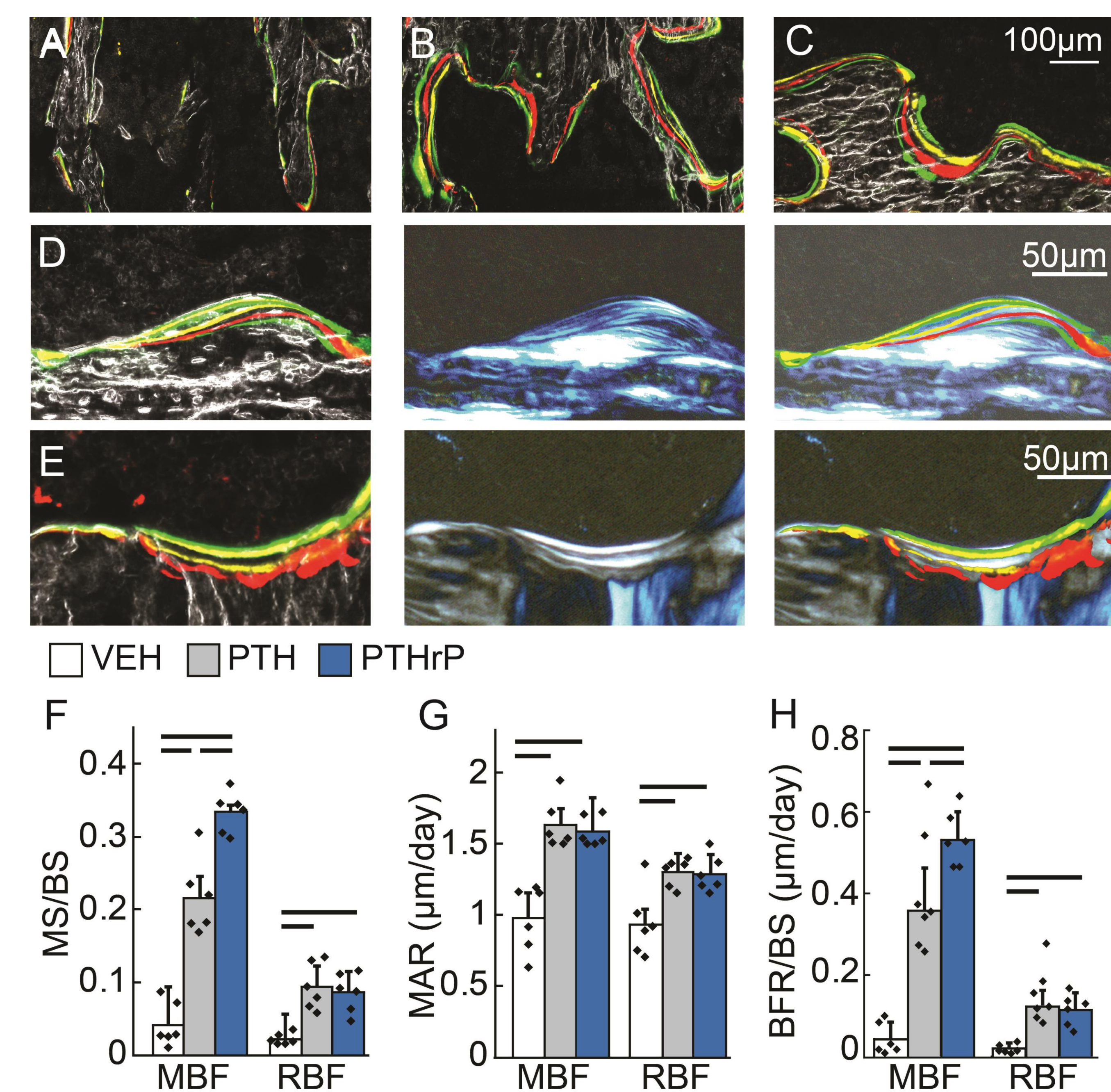


**Fig.2** (A-C) Representative images of bone dynamics of (A) VEH, (B) PTH, and (C) PTHrP groups. (D-E) Representative images of (D) MBF sites and (E) RBF sites where MBF sites were identified by smooth cement lines and uniform collagen fiber alignment indicated by polarized images while RBF sites were identified by scalloped cement lines with interrupted collagen fiber alignment. (F) MS/BS, (G) MAR, and (H) BFR/BS of MBF and RBF in response to VEH, PTH, and PTHrP. Bar:  $p < 0.05$  by one-way ANOVA.

## Discussion

- VEH treatment → Decreased structural integrity of trabecular bone microarchitecture, despite increase in MBF and RBF
- PTH and PTHrP → Enhanced structural integrity of the trabecular network by inducing greater MBF and RBF compared to VEH
- More effective improvement in trabecular bone volume and microarchitecture with PTHrP vs. PTH due to activation of more MBF surfaces
- Rate of mineral deposition not a contributing factor to improvement in trabecular bone
- Clinically, PTHrP administered at 4x the dose of PTH [4] → Expect further improvements in trabecular microarchitecture and greater induction of MBF

### Conclusions

- Both MBF and RBF contribute to the improved trabecular bone microarchitecture in response to anabolic agents
- PTHrP (clinically abaloparatide) is more efficient at stimulating MBF and improving trabecular bone microarchitecture than PTH (clinically teriparatide) in OVX rats
  - More work is needed to confirm this result in humans

## References

- [1] Lindsay *et al.* J Bone Miner Res, 2006; [2] Kobayashi *et al.* Bone, 2003; [3] Jee *et al.* J Musculoskelet Neuronal Interact, 2007; [4] Leder *et al.* JCEM, 2015.

## Acknowledgements

NIH/NIAMS K01-AR066743, NSF #1661858, Penn Center for Musculoskeletal Disorders (P30-AR069619), and 5-T32-AR007132.